Finisterra, XXVII, 53-54, 1992, p. 63 - 78

BURNED AREA MAPPING WITH CONVENTIONAL AND SELECTIVE PRINCIPAL COMPONENT ANALYSIS

JOSÉ M. C. PEREIRA (1)

INTRODUCTION

Wildfires are an important cause of land cover change in many rural areas of Portugal. During the last fifteen years (1978-1992), wildfires burned approximately 1,263,000 ha of forests, shrublands and rangelands, which corresponds to about 14% of the total area of the country. For the last three years, the Direcção-Geral das Florestas (the government agency responsible for the forest sector) has estimated the extent of burned areas by visual interpretation of Landsat TM imagery. Although comparisons with field data suggest that the technique is reasonably effective, automated multitemporal image processing may help overcome some typical problems in burned area mapping either by means of visual interpretation, or in preparation for automated classification. However, these methodologies require access to expanded hardware facilities, since automated image processing implies the performance of analytical operations that generate relatively large amounts of intermediate data. In the specific case of the Portuguese rural landscape, some of these operations will be necessary to deal with confusion problems generated by rugged topography, which causes deep shading of steep slopes with northern and northwestern aspect.

Multitemporal image processing techniques were primarily devised for change detection, and are usually combined with multivariate statistical analysis procedures that enhance their

(1) Assistant Professor, Dept. Engenharia Florestal, I.S. Agronomia, Tapada da Ajuda, 1399 Lisboa Codex, Portugal. Tel. 3511 363 46 67 Fax. 3511 364 50 00

capabilities. The present paper applies some of those techniques to burned area mapping, using a specific example of a large wildfire that took place in a mountainous area of Central Portugal, in July, 1990.

STUDY AREA AND DATA DESCRIPTION

The data used in this study are from the Landsat-5 TM sensor, gathered over Central Portugal in November 1989 and November 1990. Table 1 contains the information on dates and solar position for both Landsat passes. A full Landsat scene covers a square area of 185km by 185km, but for the present case study a data subset of 18.75km by 11.82km was used. With the Landsat TM ground resolution of 30m, this represents a database with 625 columns and 394 rows, for a total of 246,250 grid cells, or pixels. All seven TM spectral bands were available, although the thermal band (band 6) was not used.

Table 1. Exact timing and solar position for both Landsat passes, as read from the CCT tape headers.

Date	Hour (GMT)	Sun zenith angle (°)	Sun azimuth angle (°)
11.09.1989	10:33:13	64.07	64.07
11.12.1990	10:38:35	61.74	61.74

The study area, with an elevation range of 269m to 1180m is located south of Arganil and contains Pampilhosa da Serra at its southern edge. The Santa Luzia dam, on Ribeira da Pampilhosa, is located at the eastern edge, and Rio Ceira runs through the northern part of the study area. Prior to the fire uncultivated shrublands were the dominant land cover type. Pine and eucalyptus plantations are also present and small agricultural fields are found near the villages, at the bottom of the wider, more fertile valleys.

SPECTRAL BEHAVIOUR OF BURNED AREAS

Wildfires change land cover through burning of different vegetation types, leaving the surface covered with a charcoal residue, as well as partially burned plant parts and patches of more or less intact vegetation. The spectral consequences of these processes are complex, since charcoal residues have a typically very low and flat spectral reflectance curve in the visible and near-infrared regions of the spectrum (TANAKA *et al.*, 1983), while scorched vegetation reflectance increases in the visible and decreases in the near-infrared wavelengths (CHUVIECO and CONGALTON, 1988). This allowed JAKUBAUSKAS *et al.* (1990), in their study of vegetation change after an intense forest fire in a Michigan mixed forest dominated by *Pinus banksiana*, to create a map of fire severity with three classes (severe, moderate, and light) based on the direct proportionality between fire intensity and decrease in infrared reflectance.

Very dark scars are visible shortly after wildfires, while the charcoal residue is still abundant. This residue is gradually dispersed by wind and rainfall, and the fire scar becomes lighter, more reflective, and less contrasting with the surrounding vegetation. This pattern was observed by FULLER and ROUSE (1979) who analysed Landsat MSS images of a sequence of fire scars up to 80 years old, in a subarctic spruce lichen woodland located in Saskatchewan, Canada. HALL *et al.* (1980), also using Landsat MSS, detected a similar pattern of increased reflectance of the burned area during the first year after a 48km^2 tundra wildfire in Alaska.

Obviously, it is much easier to detect fire scars shortly after the fire, while they are still very dark. However, if the goal is not to study a specific fire event, but to map areas burned over an entire fire season, it is more cost-effective to purchase satellite imagery from a single date, after the end of the "normal" fire season. In the case of the average fire season in Portugal, the optimum period for imagery acquisition is probably late October or early November, to cover a fire season that usually starts around late May or early June (scattered small fires may occur as early as March, in drier years). This means that when the first fire scars of the season are imaged, they will be more than six months old and will have lost most of the charcoal residue.

It is, then, useful to implement change detection techniques capable of enhancing the fire scar signal and facilitate their identification and mapping, either by visual interpretation or by automated

classification procedures. Under a continued program of yearly burned area mapping, it is possible to use images from previous years to define baseline conditions, and apply image differencing and multitemporal principal component analysis (PCA) techniques for change detection.

METHODS

Pre-processing

Image pre-processing consisted essentially of extracting the data windows from the full scenes and registering them to 1:25,000 topographic maps from the Serviço Cartográfico do Exército. Geometric correction of the imagery was performed by collecting ground control points on the topographic maps and on the images. The images were warped to fit the topographic maps by using nearest-neighbor pixel resampling and a third order polynomial function.

Multitemporal PCA: the conventional approach

RICHARDS (1986) describes the principal component transformation as a redundance reduction technique that maps image data into a new and uncorrelated coordinate system. It produces a vector space in which most of the data variance is aligned with its first axis or principal component, the bulk of the remaining unexplained variance lying along the second, mutually orthogonal principal component axis, and so on. Higher than about third order principal component usually represent little variance and are often ignored in image classification procedures, thereby reducing the dimensionality of the classification space (4-dimensional with Landsat MSS, 7-dimensional with LANSDAT TM).

In multitemporal studies concerned with change detection, however, the interesting information resides exactly in higher order component, and the first principal component is the least useful one. RICHARDS (1984) explains that this is due to high correlation between dates for regions that remain constant, and low correlation associated with regions that change through time. A pre-requisite for the technique to work properly is that a large part of the variance in multitemporal imagery be associated with unchanging land cover

types (BYRNE *et al.*, 1980; RICHARDS, 1984). When this pre-requisite is met, regions of local change are enhanced in higher level components. Figure 1 (adapted from RICHARDS, 1986) provides a graphical explanation of these principles.

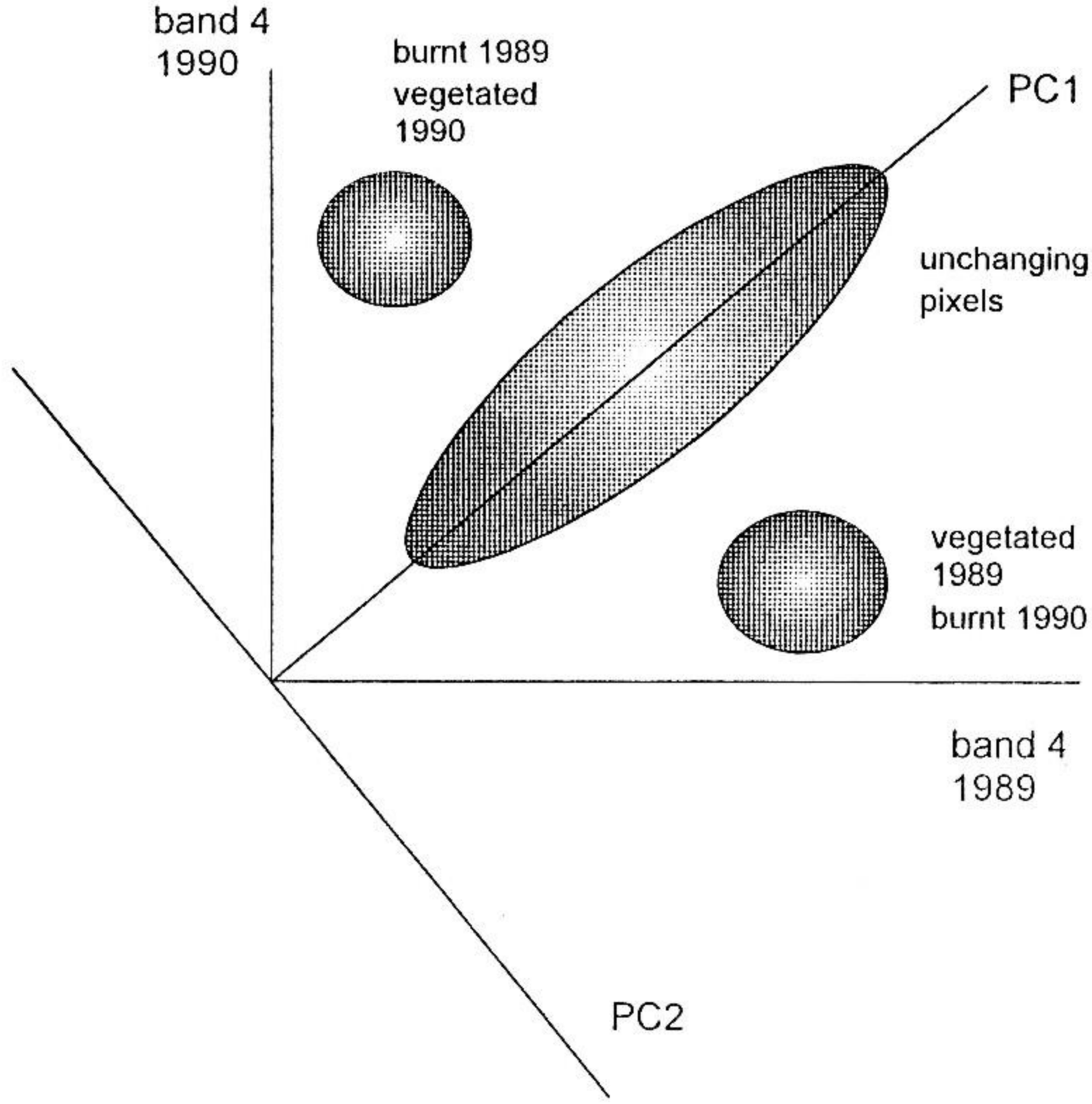

Figure 1 – Hypothetical two-date bidimensional Landsat TM space, showing the scatter of pixels associated with unaltered and changing regions. Separability of pixel clusters is enhanced by projection onto PC2 (adapted from J. A. RICHARDS, 1986, Fig.11.6, p.243).

For the present study, multitemporal PCA was performed using the 12 reflective bands of the images for the two dates, and the first five principal components were extracted. All PCAs reported here were applied to standardized data (i.e., using the correlation matrix and not the covariance matrix) from the entire study area, according to the recommendations of FUNG and LEDREW (1987).

Selective PCA

CHAVEZ and KWARTENG (1989) refer two problems with conventional PCA, namely the mapping of interesting information to high order components, unused in three band colour composites, and difficulty of interpretation and classification of such images. They propose a modification of PCA, designated selective PCA, in which only part of the available satellite bands are used as input. When the goal of selective PCA is dimensionality reduction, the inter-band correlation matrix is used to identify pairs of highly correlated bands for input.

Alternatively, one may be interested in information that is unique to a given spectral band, rather than in the overall spectral behaviour of different cover types, in which case selective PCA is performed on pairs of bands with low to medium correlation. This technique, called spectral contrast mapping (CHAVEZ and KWARTENG, 1989) relies on the concept that by using only two bands as inputs, the information that is common to both bands will be mapped to the first component, and information that is unique to either band will show up in the second component. This also makes the imagery much easier to interpret, since the relevant output of the procedure is a single grey-tone image.

In the present case, Landsat TM band 4 for both dates was used as input to selective PCA, therefore simplifying the conventional PCA procedure of using all six TM reflective bands. This requires much less disk storage space and significantly speeds up computation. Such an approach had been anticipated by RICHARDS (1984) in his multitemporal analysis of land cover changes associated with a wildfire. He performed a PCA of the two bands 7 in a pair of Landsat MSS images, and indicates that PC2 summarizes all the interesting changes.

RESULTS AND DISCUSSION

Conventional PCA

Table 2 summarizes the results of the PCA. Table 2a shows the eigenvalues for each PC, and their associated percentages of explained variance. It can be seen that the first 4 PC of the PCA performed on the 12 reflective bands of the pre- and post-fire images explain 93.68% of the observed variance. Table 2b displays the loadings of

the 12 Landsat bands on each of the first 4 PC. These 4 PC are shown in Figure 2a–d. PC1 (fig.2a) is clearly dominated by topographic, illumination–related information, in agreement with the findings of BYRNE *et al.* (1980) and RICHARDS (1984). This is made evident by comparison with fig.2e, which shows an analytical hill

Table 2a

Component	Eigenvalue	% variance
1	8.23	68.58
2	1.88	15.63
3	0.75	6.28
4	0.38	3.19
5	0.23	1.88
6	0.17	1.38
7	0.12	0.97
8	0.10	0.85
9	0.06	0.53
10	0.04	0.33
11	0.03	0.21
12	0.02	0.18

Table 2b

	Loading			
Band	Compo–nent 1	Compo–nent 2	Compo–nent 3	Compo–nent 4
1 (1989)	0.783	0.488	–0.181	–0.056
2 (1989)	0.847	0.448	–0.103	–0.134
3 (1989)	0.837	0.453	–0.218	–0.050
4 (1989)	0.711	0.158	0.564	–0.361
5 (1989)	0.912	0.230	0.031	0.012
7 (1989)	0.841	0.333	–0.218	0.175
1 (1990)	0.839	–0.462	–0.107	0.025
2 (1990)	0.890	–0.383	–0.073	0.069
3 (1990)	0.859	–0.454	–0.121	0.012
4 (1990)	0.730	0.188	0.500	0.410
5 (1990)	0.873	–0.382	0.108	0.032
7 (1990)	0.790	–0.543	–0.045	–0.155

Table 2. Results of conventional PCA. 2a) Eigenvalues and associated percentages of explained variance; 2b) Loadings associated with the first 4 principal components shown in Figure 2.

shading model for the study area. Simulated solar zenith and azimuth angles correspond to the sun's position in November 9, 1989, which is the date of the pre-fire Landsat image. The high positive loading of all 12 bands of PC1 is also indicative of its close relationship with total image brightness.

The topographic effect is minimal on PC2 (fig.2b), where the fire scar is already well visible. However, the northwestern boundary of the fire scar is somewhat fuzzy, apparently due to confusion with some deep terrain shading present in the area (fig.2e). All 1989 bands have positive loadings on this component, while all 1990 bands except band 4 have negative loadings, which indicates that PC2 detects a contrast between the two dates. A similar effect is observed for the bands 1-4 in PC4.

PC3 (fig.2c) does not provide a clear depiction of the burned area, in spite of the almost complete absence of illumination effects. Older fire scars, in the northwest and southeast corners of the study area, and smaller scattered ones show up clearly as darker patches. This is the PC where those revegetating scars are more obvious. No sign reversal is observed for the loadings of 1989 and 1990 bands on PC3, indicating that, like PC1, it is also representing essentially unaltered features, and not landscape changes. The high positive loadings of band 4 for both dates gives PC3 an overall bright appearance.

The larger, more recent burned area is again distinguishable in PC4 (fig.2d), where it reveals higher variability of grey tones than in PC2. This may be related to more subtle scar features, dependent on previous land cover and fire intensity. Loadings for all bands except band 5 suffer sign reversals between dates, which explains PC4's ability to detect the fire scar.

The fact that the burned area becomes obvious in PC2, while both BYRNE *et al.* (1980) and RICHARDS (1980) report this feature only in PC3 and PC4 may be due to the fact that it occupies a larger proportion of the study area than what would be ideal for a multitemporal PCA. Another possible contributing factor is that the PCA reported here was performed with Landsat TM imagery, that has 6 reflective bands per image. Two of these are mid-infrared bands, not available in the Landsat MSS imagery used by BYRNE *et al.* (1980) and RICHARDS (1984), and where the burned area also has a relatively strong signal.

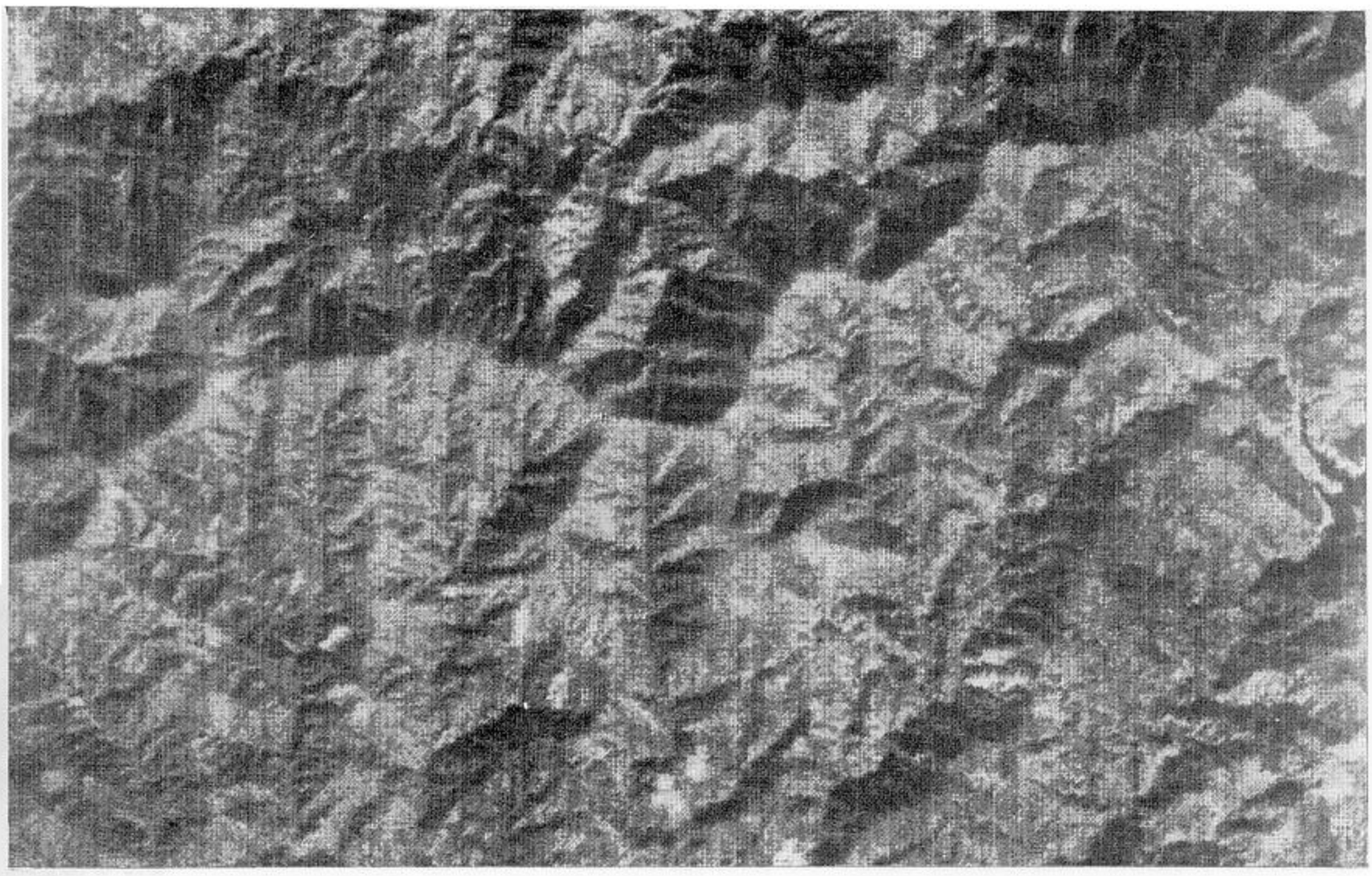

Figure 2a – PC1

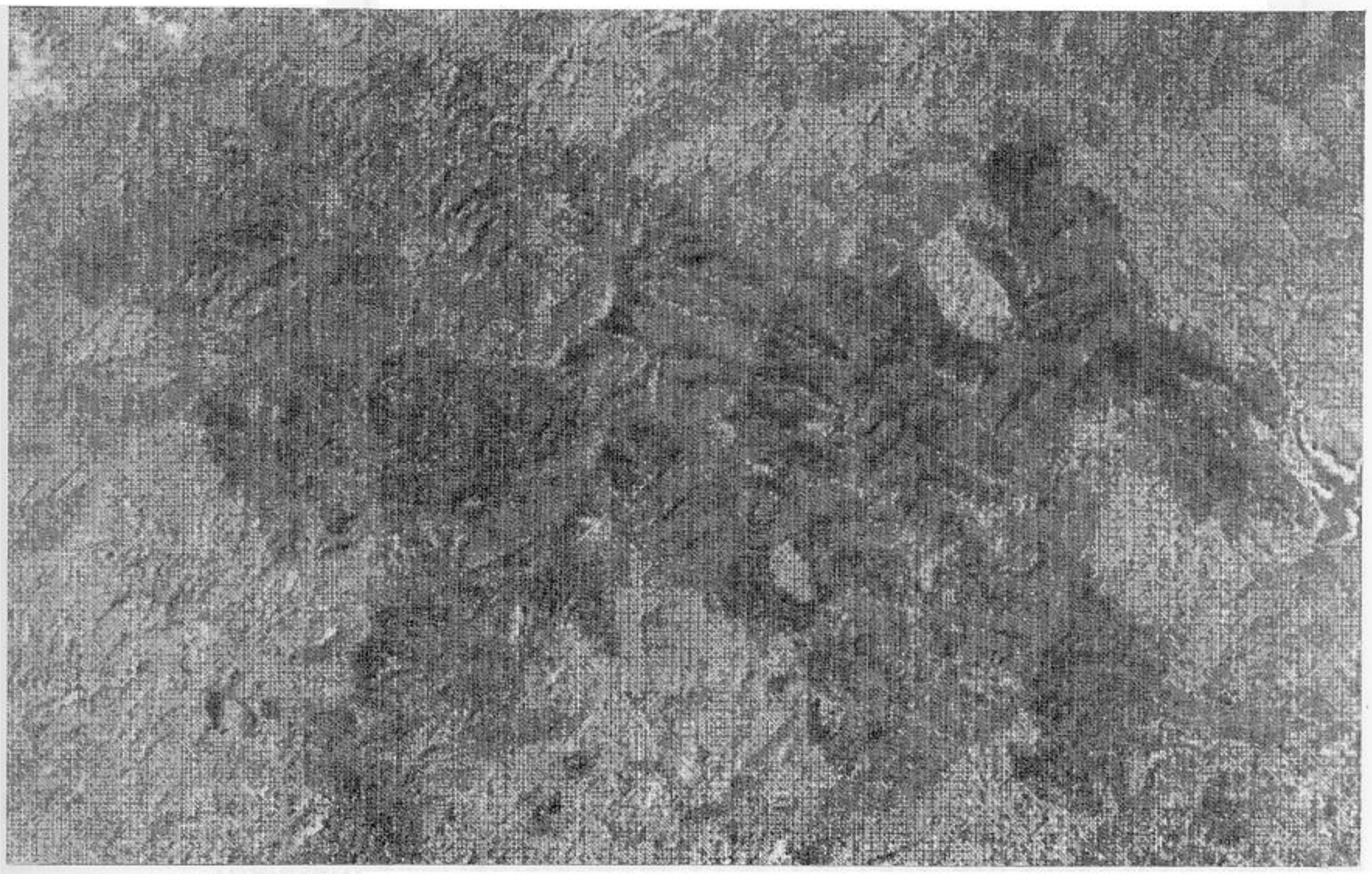

Figure 2b – PC2

Figure 2c – PC3

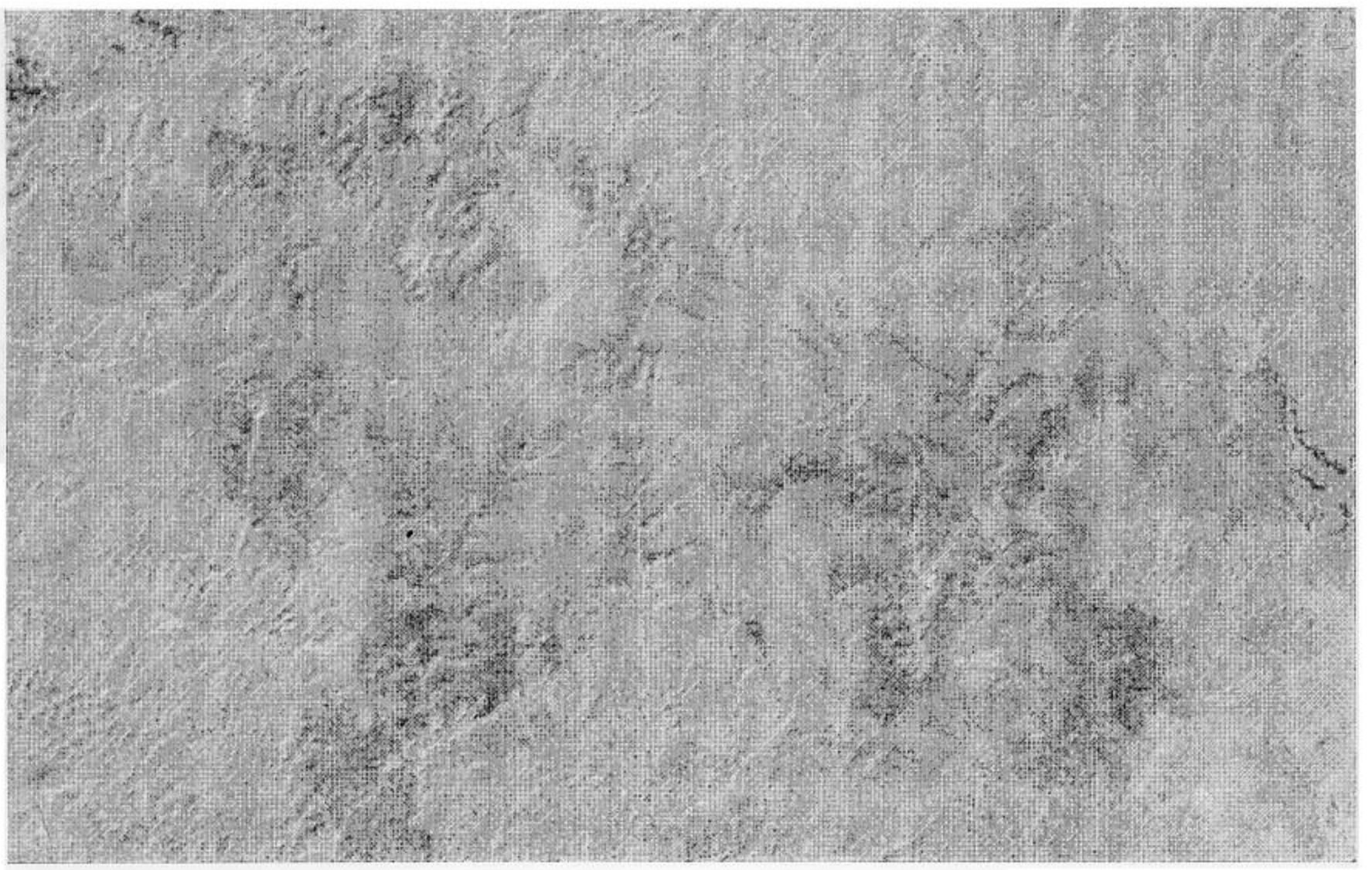

Figure 2d – PC4

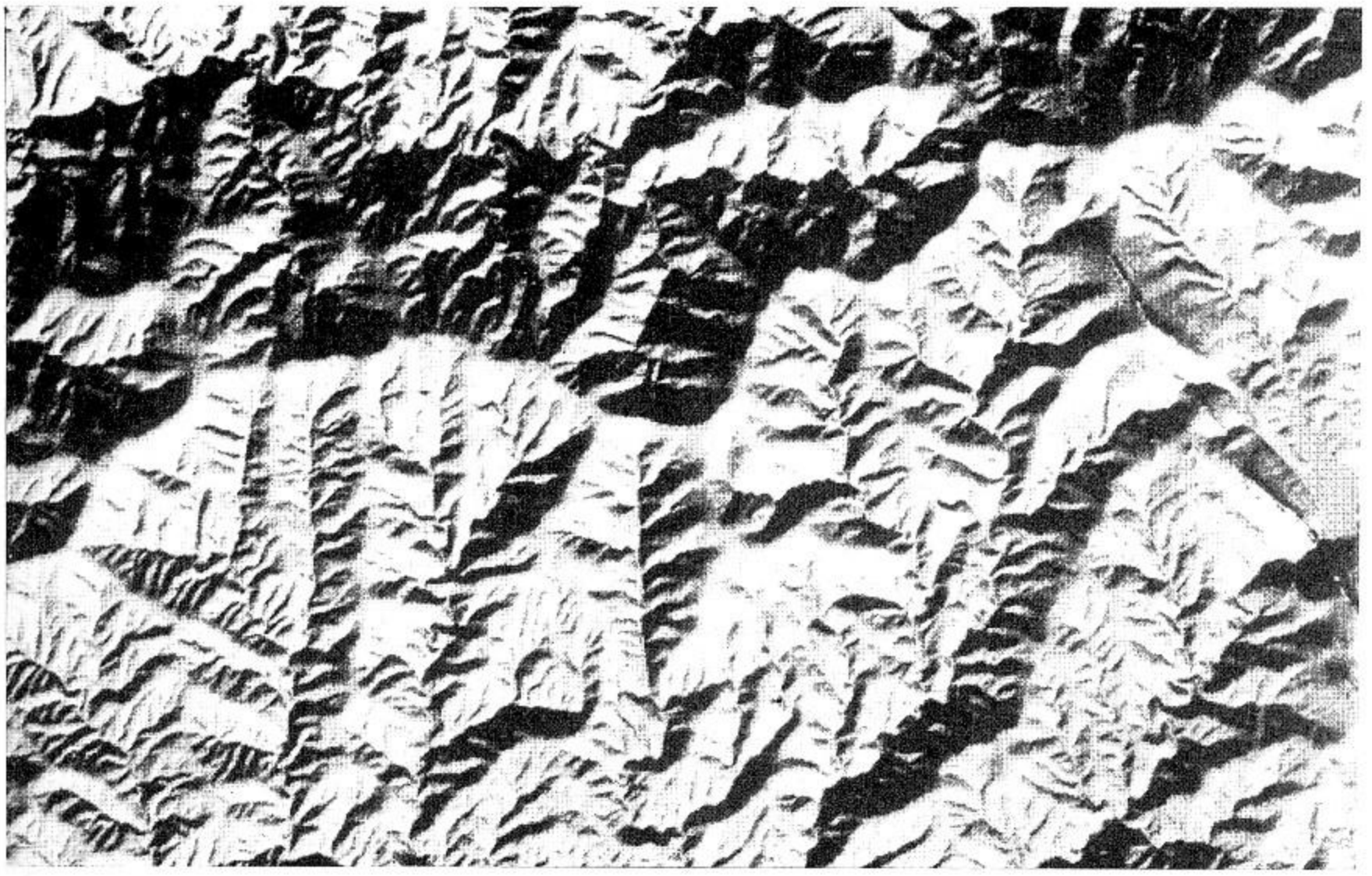

Figure 2e

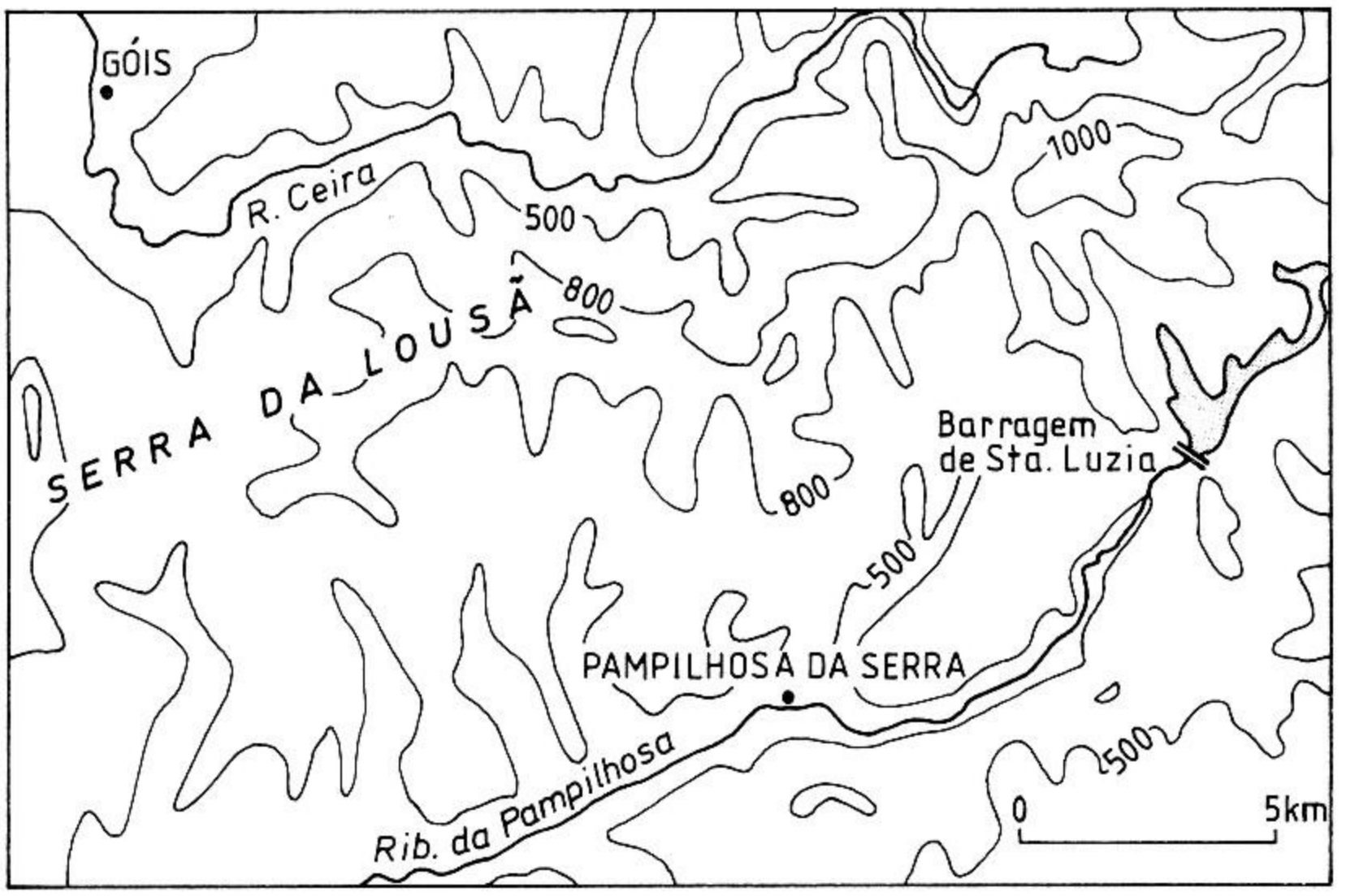

Figure 2 – Images of the first four principal components obtained with multitemporal conventional PCA. 2a) PC1; 2b) PC2; 2c) PC3; 2d) PC4. PC2 and PC4 detect land cover change and show fire scar. 2e) Analytical hill shading of study area at 10:33 AM, November 9, 1989 (sun zenith angle=64.07°, sun azimuth angle=152.51°).

Selective PCA

Selective PCA was performed on the Landsat TM bands 4, for both dates (fig.3a–b). The resulting PC1 (fig.4a) is very similar to PC1 of the conventional PCA (fig.2a), depicting primarily topographic features of the study area. PC2 of the selective PCA (fig.4b) effectively detects the land cover changes due to fires and looks similar to PC4 of the conventional PCA (fig.2d), although with a slightly enhanced contrast relatively to the unchanged background. The visual quality of the results is comparable to that obtained with the conventional procedure of using all reflective bands, making selective PCA a more attractive procedure, since it requires much smaller amounts of data and processing time.

CONCLUSIONS

Conclusions can be drawn regarding the relative performance of the methodologies tested for enhancing the separability between burned areas and the surrounding unaffected landscape, while minimizing confusion due to topographic effects. Conventional PCA was comparatively less effective, although the large fire scar is visible in PC2 and PC4. Selective PCA, requiring the use of only two weakly correlated spectral bands, one per date, is more effective than conventional PCA and clearly more efficient from a computational standpoint.

Table 3a

Component	1	2
Eigenvalue	1.68	0.32
% variance	83.84	16.16

Table 3b

	Loading	
Band	Component 1	Component 2
4 (1989)	0.916	−0.402
4 (1990)	0.916	0.402

Table 3 – Results of selective PCA. 3a) Eigenvalues and associated percentages of explained variance; 3b) Loadings associated with the two principal components shown in Figure 4.

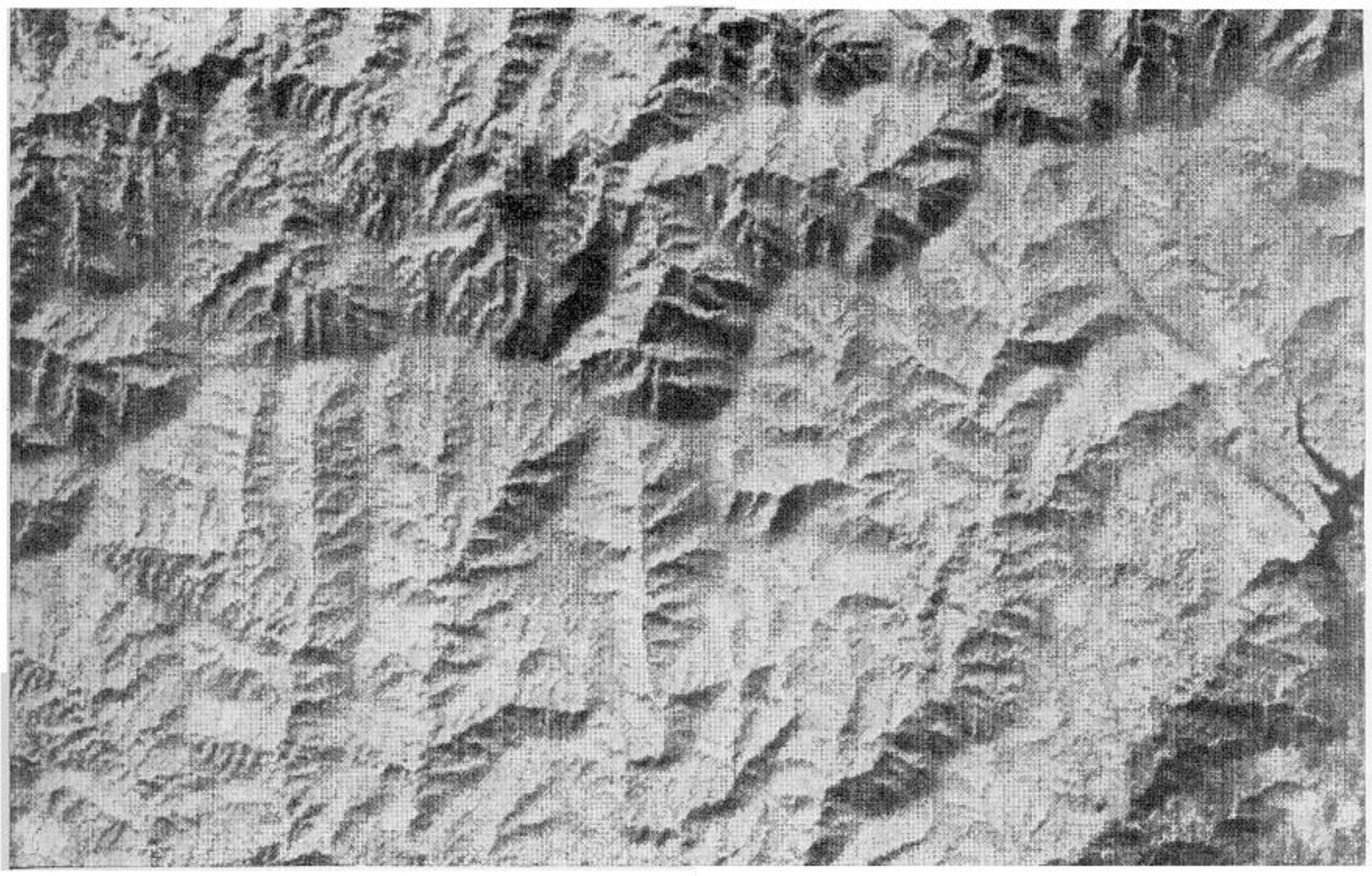

Figure 3a – Pre-fire

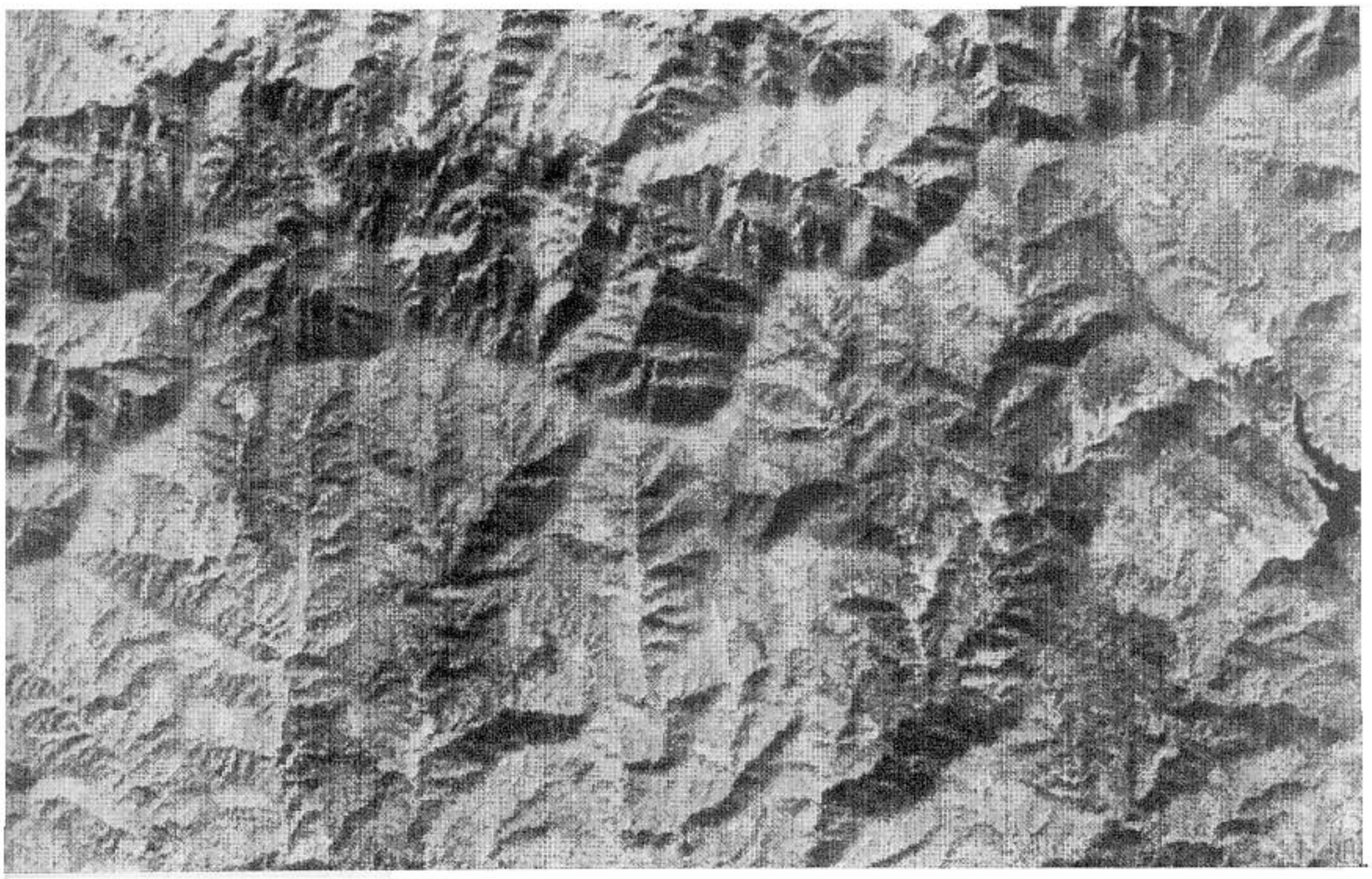

Figure 3b – Post-fire

Figure 3 – Landsat TM band 4 (near-infrared). 3a) Pre-fire, November 9, 1989; 3b) Post-fire, November 12, 1990.

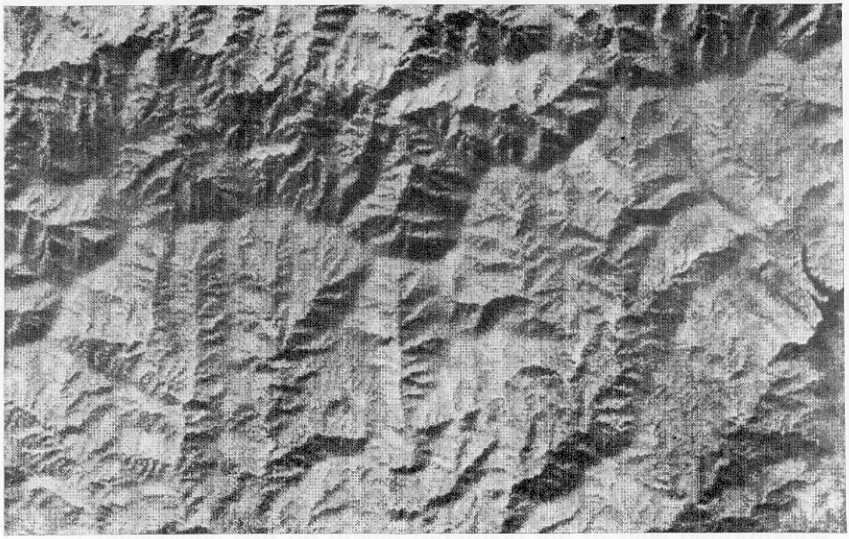

Figure 4a

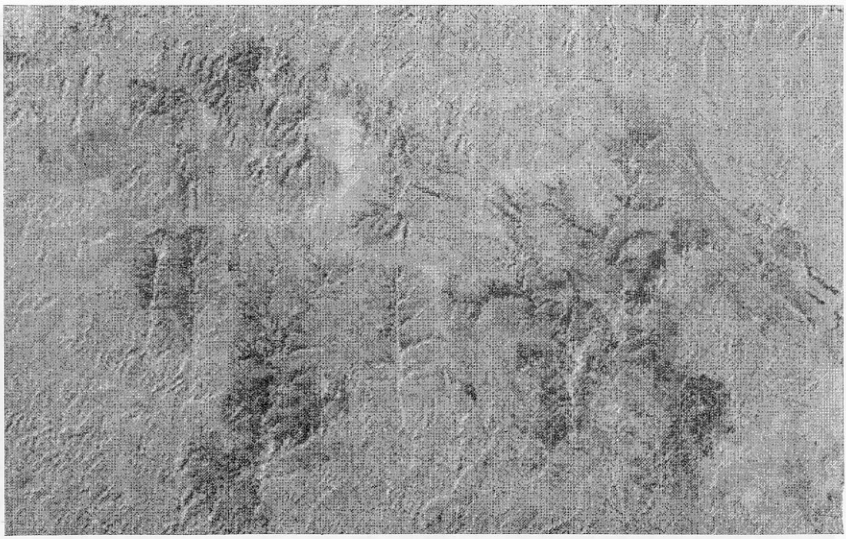

Figure 4b –

Figure 4 – Multitemporal selective PCA images. 4a) PC1, quite similar to PC1 of the conventional PCA; 4b) PC2 contains most of the information on land cover change, depicting fire scar.

Acknowledgments

Funding for this work was provided by Junta Nacional de Investigação Científica e Tecnológica (JNICT, Project PMCT AGR/604/90), SOPORCEL, CELBI, and Comissão Nacional Especializada para os Fogos Florestais (CNEFF). I am also very grateful to Engs. Leonor Cadete and Rui Almeida, of Centro Nacional de Informação Geográfica (CNIG), who set up the remote sensing and GIS database for the Pampilhosa da Serra fire study.

REFERENCES

BYRNE, G. F., P. F. CRAPPER AND K. K. MAYO (1980) – Monitoring land-cover change by principal component analysis of multitemporal Landsat data. *Remote Sensing of Environment*, 10: 175–184.

CHAVEZ, P. S.; A. Y. KWARTENG (1989) – Extracting spectral contrast in Landsat Thematic Mapper image data using selective principal component analysis. *Photogrammetric Engineering and Remote Sensing*, 55: 339–348.

CHUVIECO, E.; R. G. CONGALTON (1988) – Mapping and inventory of forest fires from digital processing of TM data. *Geocarto International*, 4: 41–53.

FULLER, S. P.; W. R. ROUSE (1979) – Spectral reflectance changes accompanying a post–fire recovery sequence in a subarctic spruce lichen woodland. *Remote Sensing of Environment*, 8: 11–23.

FUNG, T.; E. LEDREW (1987) – Application of principal component analysis to change detection. *Photogrammetric Engineering and Remote Sensing*, 53: 1649–1658.

HALL, D. K.; J. P. ORMSBY; L. JOHNSON; J. BROWN (1980) – Landsat digital analysis of the initial recovery of burned tundra at Kokolik River, Alaska. *Remote Sensing of Environment*, 10: 263–272.

JAKUBAUSKAS, M. E.; K. P. LULLA; P. W. MAUSEL (1990) – Assessment of vegetation change in a fire–altered forest landscape. *Photogrammetric Engineering and Remote Sensing*, 56: 371–377.

RICHARDS, J. A. (1984) – Thematic Mapping from multitemporal image data using the principal components transformation. *Remote Sensing of Environment*, 16: 35–46.

RICHARDS, J. A. (1986) – *Remote Sensing Digital Image Analysis: an Introduction*. Springer–Verlag, Berlin.

TANAKA, S.; H. KIMURA; Y. SUGA (1983) - Preparation of a 1:25,000 Landsat map for assessment of burnt area on Etajima island. *International Journal of Remote Sensing*, 4: 17-31.

SUMMARY

Burned area mapping with conventional and selective principal component analysis

Conventional principal component analysis and selective principal component analysis are presented and compared as multitemporal analysis techniques for burned areas mapping. These two methodologies are applied to Landsat - 5TM imagery of a large wildfire that occurred in Central Portugal, in July of 1990. Results are compared and conclusions are drawn that indicate higher effectiveness and computational simplicity of the selective approach.

Key-words: principal component analysis, burned areas mapping, Central Portugal.

RESUMO

Representação cartográfica de áreas ardidas recorrendo à análise de componentes principais (convencional e selectiva)

São apresentadas duas técnicas de análise multitemporal para a representação cartográfica de áreas ardidas: análise de componentes principais convencional e análise de componentes principais selectiva.

As duas metodologias foram aplicadas a imagens Landsat - 5TM referentes a um grande incêndio florestal ocorrido no centro de Portugal em Julho de 1990.

Os resultados são comparados e as conclusões apontam a análise de componentes principais selectiva como a técnica que proporciona melhores resultados finais, ao mesmo tempo que implica uma menor complexidade de tratamento informático.

Palavras-chave: análise de componentes principais, representação cartográfica de áreas ardidas, centro de Portugal.